Neural Network Based Real-time Heart Sound Monitor Using a Wireless Wearable Wrist Sensor

W.Y. Shi and J.-C. Chiao
Department of Electrical Engineering
The University of Texas at Arlington
Arlington, TX, 76019, USA
wenyuan.shi@mavs.uta.edu

***Abstract*—The paper presents a new method to estimate acoustic parameters *S*1 and *S*2 of the heart sounds using a wearable wrist sensor based on the neural network technique. Using the new method, the heart conditions can be analyzed and monitored in real time and potentially in a long term with a wrist device. The velocities and time delays of the cardiac pulse waves in blood vessels were experimentally acquired and calculated at different artery locations on the human body. Signal attenuation of the pulses from the heart to the wrist artery was analyzed and a pulse-waveform transfer model in artery was proposed. A neural network with two layers and 500 tansig neurons was employed to emulate the inverse acoustic transfer function from the wrist to heart. Comparisons between the parameters of the original heart sounds and estimated cardiac sounds were made to verify the accuracy of the neural network. It is encouraging to find that the acoustic properties of the original and estimated heart sounds have an accuracy up to 100% and the heart rates have an accuracy up to 99%. Using the trained neural network, heart sounds were estimated from the wrist artery by connecting the wrist sensor to a Bluetooth audio module to implement a wearable heart sound estimator. Performance of the new estimation method was verified. The proposed wrist sensor aims as a wireless wearable monitor on wrists for continuous and long-term medical diagnosis and athlete performance monitoring.**

Keywords—Wireless sensor networks, Stethoscope, Digital signal processing, Neural network.

I. INTRODUCTION

Wearable Holter monitor is usually used to record heart activities. However, six to ten wet electrodes must be attached to the skin on chest with wires around the body [1], causing inconvenience and discomfort for patient during long-term monitoring [1]. On the other hand, stethoscope has been an important device for diagnosing heart diseases. Stethoscopes can pick up murmurs from echoes, especially those occur irregularly. However, it is difficult to adhere a stethoscope on chest as a wearable sensor due to its size and weight. Additionally, speaking and breathing sounds during the recording affect the quality of the recorded data. Currently, most convenient wearable devices are designed for the wrist and can only detect artery pulses by measuring strain or pressure changes to calculate heartbeats.

We believe that more information about the heart and blood vessels can be provided along the artery locations. The velocities and delays of the pulse waveforms in the arteries can further provide information about blood pressures [2], [3]. The velocities of the cardiac pulse waves in body have been reported as 4−10 meters per second [2]. Phonocardiography [4] and digital stethoscopes with mathematical decomposition methods have been developed [5]. Mandal *et al.* presented detailed measurement results of the velocities and delays of arterial pulse waves with two microphones attached to the subject's neck and wrist [3]. The correlation between the pulses detected at neck and wrist was studied.

In our previous work, the Short Time Fourier Transform (STFT) method has been proposed to determine key parameters such as the occurrence times of heart sounds *S*1 and *S*2 recorded from the heart [6]. These parameters can be displayed graphically in real time as visual features for the heart sounds to provide a quick diagnosis tool. The technique was demonstrated with a digital wireless microphone adhered on the chest. Although it is feasible and suitable to conduct such measurements in clinics, it is not convenient for daily uses at home, work or in a training facility. It will be nice if the similar features can be detected directly with a convenient and comfortable wrist wearable.

When blood flows from the heart to the wrist artery, the blood pressures and cardiac pulse waves change, which are expected to be a compound and nonlinear process. The cardiac pulse waves can be transferred into sound signals which can be detected by condenser microphones. However, the relationship to the original heart sounds are complex. We propose to find the inverse function for the pulse sounds between two locations along the same artery to restore or estimate the heart sounds with the recording from a wrist artery.

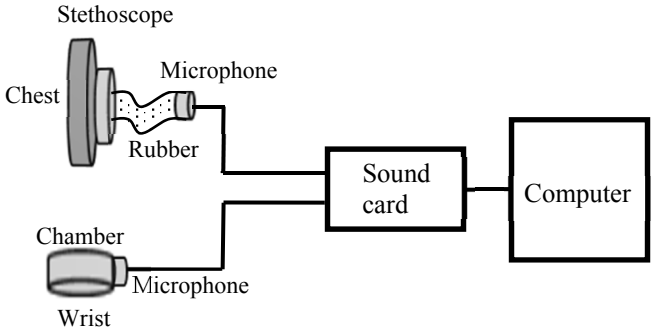

Fig. 1. Experimental configuration: A small air chamber and a stethoscope head are connected to two condenser microphones via a computer sound card for digital recording.

978-1-5090-2757-6/16/$31.00 © 2016 IEEE

Artificial neural networks can emulate complex functions. A trained neural network may imitate the inverse function of the pulse wave sounds from the blood flow in the artery. In our work, we further used a Bluetooth-connected audio device to connect the wrist sensor to a computer. In such a case, the heart sounds can be estimated without an attachment on the chest.

A wearable wireless sensor can be used to conveniently monitor a cardiac patient's daily health without constraints or limitation on mobility. In this work, such a wrist sensor was designed and implemented, with low-power consumption and high-connectivity wireless communication in mind, for continuous recording with comfort.

II. Experiment Configuration

The proposed wrist sensor to record wrist artery sounds consists of a 3D-printed air chamber with a diameter of 15 mm and a thickness of 5 mm and a PUM-5250 condenser microphone (PUI Audio, Inc.). In order to compare the heart sounds, a stethoscope head is reconfigured and connected to a condenser microphone. A computer with a sound card is used to record both heart and wrist sounds simultaneously. The sound card gain is set at 25. The analog to digital conversion (ADC) of the sound card is at 44,100 samples/second with a 16-bit resolution. The configuration is shown in Fig. 1. The air chamber was strapped on the wrist to acquire wrist artery sounds and the stethoscope diaphragm was placed on the chest to acquire heart sounds simultaneously.

III. Pulse Wave Sound Travel Model in Artery

Pulse wave sounds at heart and the left subclavian artery were simultaneously acquired by placing the stethoscope head on the chest and the air chamber on top of the left neck where was estimated to be near the subclavian artery location. The results are shown in Fig. 2(a) and (b). The air chamber was moved on the left elbow to simultaneously acquire the pulse sounds from the radial artery around the left elbow joint, roughly mid-point of the brachial artery along the arm. The result is shown in Fig. 2(c). The chamber then was placed on the wrist to simultaneously acquire the heart sounds and pulse wave sounds at wrist radial artery and the result is shown in Fig. 2(d).

Important acoustic properties of the heart sounds, the occurring time of *S*1 and *S*2, as shown in Fig. 2(a), can be calculated by the time-frequency peaks [6]. The acoustic properties, *S*1 and *S*2, transient heart rate, and ratio of *S*1 to *S*2 are listed in Table I, which can be used to continuously monitor for arrhythmia and other heart diseases, such as that the ratio of

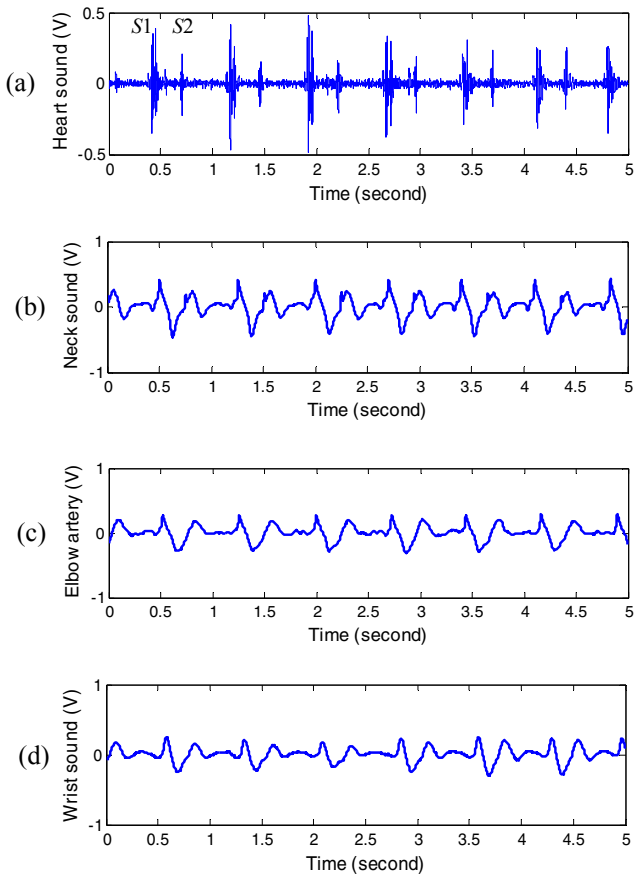

Fig. 2. Attenuation and delays of sounds from the heart to the wrist artery. (a) Heart sounds. (b) Neck subclavian artery sounds with an average delay of 0.05 seconds from the heart sounds, (c) Sounds of elbow brachial artery with an average delay of 0.095 seconds from heart sounds, (d) Wrist radial artery sounds with an average delay of 0.155 seconds from heart sounds.

*S*1 to *S*2 displayed the highest correlation with the systolic blood pressure [7].

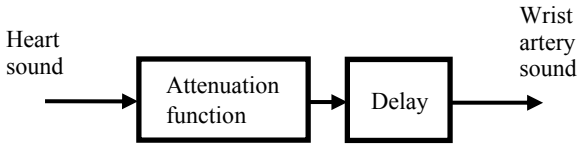

Fig. 3. The travel model of pulse wave sounds in blood vessels.

TABLE I. Acoustic Properties of the Heart Sound

Heart sound segment (n)	1	2	3	4	5	6	Mean
Occurring time of *S*1 (seconds)	0.42	1.17	1.92	2.68	3.42	4.13	N/A
Occurring time of *S*2 (seconds)	0.71	1.46	2.21	2.96	3.70	4.41	N/A
$S1(n+1) - S1(n)$ (seconds)	0.75	0.75	0.76	0.74	0.71	N/A	0.74
Heart rate (bpm)	N/A	80.00	80.00	78.95	81.08	84.51	80.91
$S2(n) - S1(n)$ (seconds)	0.29	0.29	0.29	0.28	0.28	0.28	0.28
*S*1 to *S*2 ratio $\frac{S2(n)-S1(n)}{S1(n+1)-S1(n)}$	38.67%	38.67%	38.16%	37.84%	39.44%	N/A	38.56%

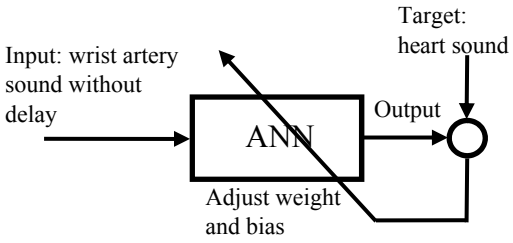

Fig. 4. Neural networks for training the inverse attenuation function.

The sound waveforms attenuate with the increased time delays, as shown in Fig. 2, from the heart to the left subclavian artery, connecting from the heart and the neck, to the brachial artery, connecting to the elbow, and radial artery on the wrist. The sound waveforms at the blood vessels are very different from the sound waveform at chest because high frequency components of the pulse wave were absorbed in the travel process. The sounds travel in blood vessels may be modeled with a time delay block and an attenuation function block as shown in Fig. 3.

Time delay of the cardiac pulse wave sounds between various arteries and the heart can be estimated by pulse peaks in the time domain [3]. The sound delays of various arteries are estimated by time-frequency peaks using Short-Time Fourier Transform (STFT) which can give accurate transient occurrence times of *S*1 and *S*2. The estimated time delay from the heart to the neck artery is 0.05 seconds, from the heart to the elbow artery is 0.095 seconds, and from the heart to wrist artery is 0.155 seconds. The distance measured from the subject's heart to neck is 0.25 m, 0.48 m, from the heart to elbow, and 0.78 m from the heart to wrist. Average velocity of the subject the cardiac pulse wave then can be estimated as about 5 m/s [2].

IV. Neural Network

A two-layer feed-forward backpropagation neural network [7] was employed and trained, as shown in Fig. 4，which has a hidden layer with 500 tansig (hyperbolic tangent sigmoid

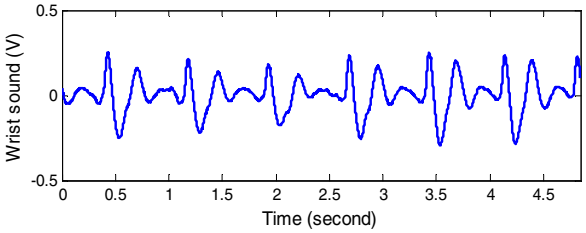

Fig. 5. Wrist artery sounds as the input to the trained network.

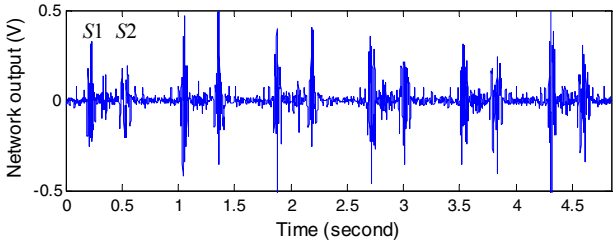

Fig. 6. Estimated heart sounds by the trained network.

transfer function) neurons and an output layer with one linear neuron. Using the Levenberg-Marquardt algorithm [8], the network was trained to adjust and update its weight and bias in every training iteration. The wrist artery sound signals shown in Fig. 5 were shifted to eliminate the estimated time delay, which then were serially fed into the neural network. The heart sound shown in Fig. 2(a) was used as the target for training the neural networks. The inverse attenuation function shown in Fig. 3 is emulated by the neural network. Training error is measured by mean squared error (MSE) expressed in (1).

$$MSE = \sqrt{\frac{1}{N}\sum_{i=1}^{N}[x_O(N) - x_T(N)]^2} \qquad (1)$$

where x_O is the network output, x_T is the target, N is sample number.

After 20 training iterations, the mean squared error between the network output and the target is less than 0.1 V.

The trained network may be used to express the inverse function of the attenuation process for estimating the heart sound. Using the wrist artery sound without the delay as input, the trained network outputs are shown in Fig. 6. The distances of *S*1 and *S*2 of the estimated heart sounds as well as detailed acoustic properties can be calculated by the time-frequency peaks again and are listed in Table II.

Compared with the waveforms shown in Figs. 2(a) and 6 as well as the acoustic properties of the heart sounds listed in Tables I and II, outputs of the trained network approximate well the original heart sounds. The mean errors in Table II, as the differences of means in Tables I and II are also small. It is clear that accurate training results have been obtained.

V. Applying to a Wearable Wireless Wrist Device

In order to verify the trained network, a wearable wireless device was used, which consisted of a small air chamber, a

TABLE II. Acoustic Properties of the Estimated Heart Sound

Heart sound segment (n)	1	2	3	4	5	6	Mean	Mean error
Occurring time of *S*1 (seconds)	0.43	1.19	1.93	2.69	3.42	4.14	N/A	N/A
Occurring time of *S*2 (seconds)	0.70	1.46	2.21	2.98	3.70	4.43	N/A	N/A
$S1(n+1) - S1(n)$ (seconds)	0.76	0.74	0.76	0.73	0.72	N/A	0.74	0.00
Heart rate (bpm)	N/A	78.95	81.08	78.95	82.19	83.33	80.90	-0.01
$S2(n) - S1(n)$ (seconds)	0.27	0.27	0.28	0.29	0.28	0.29	0.28	0.00
*S*1 to *S*2 ratio $\frac{S2(n)-S1(n)}{S1(n+1)-S1(n)}$	35.53%	36.49%	36.84%	39.73%	38.89%	N/A	37.50%	-1.06%

TABLE III. ACOUSTIC PROPERTIES OF THE VERIFIED HEART SOUND USING A BLUETOOTH MODULE

Heart sound segment (n)	1	2	3	4	5	6	Mean
Occurring time of $S1$ (seconds)	0.57	1.30	2.01	2.74	3.48	4.24	N/A
Occurring time of $S2$ (seconds)	0.89	1.61	2.30	3.03	3.77	4.54	N/A
$S1(n+1) - S1(n)$ (seconds)	0.73	0.71	0.73	0.74	0.76	N/A	0.73
Heart rate (bpm)	N/A	82.19	84.51	82.19	81.08	78.95	82.19
$S2(n) - S1(n)$ (seconds)	0.32	0.31	0.29	0.29	0.29	0.30	0.30
$S1$ to $S2$ ratio $\frac{S2(n)-S1(n)}{S1(n+1)-S1(n)}$	43.84%	43.66%	39.73%	39.19%	38.16%	N/A	40.91%

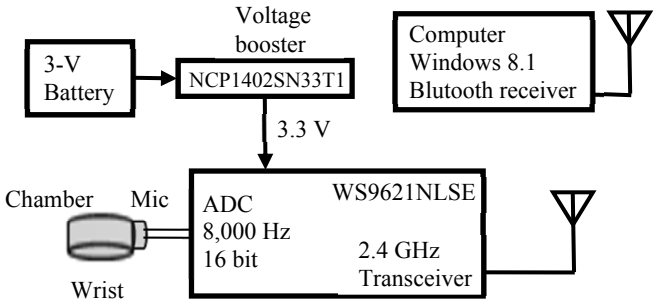

Fig. 7. A wearable wireless wrist device and system configuration.

condenser microphone, a single-channel Bluetooth audio module (with a width of 30 mm and a length of 40 mm), a 3-V cell battery (CR2032, 210 mAh), and a NCP1402SN33T1 converter IC for supplying a voltage of 3.3 V to the Bluetooth module. A computer was used to receive the wireless signals via the same transceiver module. The wearable wireless configuration is shown in Fig. 7.

The Bluetooth module used a 2.4-GHz WS9621NLSE Bluetooth IC with ADC with a 8,000 Hz sample rate and 16-bit resolution. Power consumption of the module was 8 mA. Using the CR2032 battery, the module could continuously work over 26 hours. When the small air chamber placed on left radial artery of the subject's wrist, the artery sounds can be acquired to the computer. Fig. 8 shows the signals.

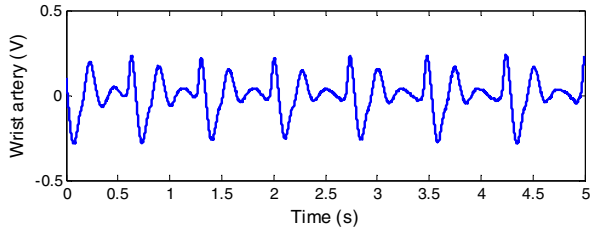

Fig. 8. Acquired wrist artery sounds by the wearable device.

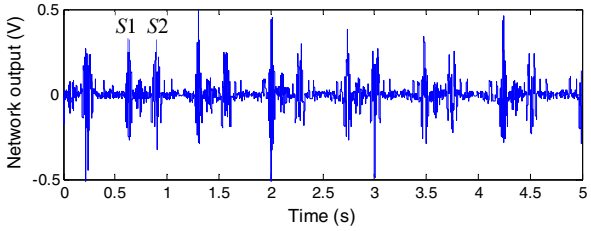

Fig. 9. Estimated heart sounds using the wearable device by the trained network.

The acquired wrist artery sounds then were used as the input signals for the trained network. The output signals of the trained network were the estimated heart sounds, as shown in Fig. 9. The distances of $S1$ and $S2$ of the estimated heart sounds, have been calculated by the time-frequency peaks again. The acoustic properties are listed in Table III. The measurement and estimation results demonstrated the feasibility of the wearable wrist sensor for heart sounds monitoring.

VI. CONCLUSIONS

A wearable wrist sensor for heart sounds monitoring has been developed to overcome the shortcomings of Holter monitors and digital stethoscopes. Using two acoustic sensors to record the cardiac sounds along the blood vessels, the sound attenuation process from the heart to differential artery locations can be modeled. Using neural network techniques, the inverse function for the cardiac sound travel can be found. With the neural network algorithm, a small in size, convenient, and wearable wrist sensor can be used to accurately estimate heart sounds. Without signals interfered by breathing, the wrist sensor provides comfort and wearability. With low-power consumption by the Bluetooth communication, the wireless wearable wrist sensor can work in real time and long term for heart monitoring.

REFERENCES

[1] J. Yoo, L. Yan, S. Lee, et al., "A wearable ECG acquisition system with compact planar-fashionable circuit board-based shirt," *IEEE Transactions on Information Technology in Biomedicine*, vol. 13, no. 6, pp. 897–902, 2009.

[2] J. C. Bramwell and A.V. Hill, "The velocity of the pulse wave in man," *Proc. Royal Soc. London*, Series B, vol. 93, no. 652, pp. 298–306, 1922.

[3] S. Mandal, L. Turicchia and R. Sarpeshkar, "A low-power, battery-free tag for body sensor networks," *IEEE Pervasive Computing,* vol. 9, no. 1, pp. 71–77. 2010.

[4] H. B. Sprague, "History and present status of phonocardiography," *IRE Trans. on Med. Electr.*, pp. 2–3, Dec. 1957.

[5] S. M. Debbal, et al, "Computerized heart sounds analysis," *Comp. in Biology and Medicine*, vol. 38, no. 2, pp. 263–280, 2008.

[6] W.Y. Shi, J. Mays and J.-C. Chiao, "Wireless stethoscope for recording heart and lung sounds," *IEEE BioWireless Conference*, Austin, TX, pp.1–4, 2016.

[7] K. H. Lim, Y. D. Shin, S. H. Park, J. H. Bae, H. J. Lee, S. J. Kim, et al. "Correlation of blood pressure and the ratio of S1 to S2 as measured by esophageal stethoscope and wireless bluetooth transmission," *Pakistan journal of medical sciences*, vol. 29, no. 4, pp. 1023–1027, 2013.

[8] B. H. Demuth and M. Beale, "Matlab neural network toolbox user's guide version 6," The MathWorks Inc., 2010.